PLASTIC FLOW AND MEMORY RULES FOR THE LOCAL STRAIN METHOD IN THE MULTIAXIAL CASE

A. Navarro

Departamento de Ingeniería Mecánica y de los Materiales, ESI, Universidad de Sevilla,
Camino de los Descubrimientos s/n, E-41092 Sevilla, Spain
E-mail: navarro@us.es

ABSTRACT
This paper describes a recently proposed theory of plastic flow which is specially suited to deal with variable amplitude multiaxial load under the common assumption of rate-independence usually employed in fatigue calculations. The theory uses, and generalizes to the multiaxial case, concepts familiar to fatigue designers acquainted with the Local Strain Approach to (low cycle) fatigue. The theory does not make use of yield or loading surfaces that move about in stress space, a common ingredient of existing cyclic plasticity theories. It uses the concept of distance in a stress space endowed with a certain metric measurable from the yield criterion. Kinematic hardening and the memory effect appear in a natural way in the framework presented. The theory is reviewed first and then the application to the classical experiment of Lamba and Sidebottom [1] is presented.

1. INTRODUCTION

The Local Strain Method constitutes nowadays a standard tool for fatigue life predictions in many industries. It has been incorporated in commercial software [2,3] and it is very well described in textbooks [4,5]. The use of the cyclic curve, the hysteresis loops, Neuber´s rule and the memory effect are explained to engineering undergraduates in many Engineering Schools these days. In the uniaxial load case, of course.

The extension of the Local Strain Method to the multiaxial case requires at least three main steps, as I see it. The first one is the development of plastic flow rules which reproduce the way we operate with hysteresis loops, cyclic curves, memory effect and so on in the simple uniaxial case. The second step would be the development of multiaxial Neuber-type rules for dealing with inelastic strains at notches. This relies heavily on the use of a theory of plasticity and hence on the previous step. There are already a number of proposals in this respect [6, 7]. The third step is probably the most difficult and it is the area where more work has been invested so far: the multiaxial cycle counting and fatigue life criteria. There are too many of them to single any one out. A comparison of several criteria is provided in [8]. They need the stresses and strains as inputs and therefore they also depend on the two previous steps.

We are concerned here with the first step. Let us just mention that currently accepted incremental plasticity theories (based on Mróz's [9] multiple surface concept or Armstrong

and Frederick's [10] non-linear hardening rules) have quite a different "feeling" or "modus operandi" from what one normally does in the Local Strain approach.

Next section reviews briefly some of the more important concepts of incremental rate-independent plasticity theories. This will put the model described in the present work in perspective.

2. CLASSICAL PLASTICITY

This section briefly reviews some of the more important concepts of incremental plasticity theories. Defining a constitutive model entails the specification of a *yield criterion*, and of *flow and hardening rules.* Moreover, when dealing with variable amplitude loads, the model requires the capability to reproduce the *memory effect.*

2.1. Yield criterion

The yield criterion defines the combination of stresses which bring about the initial production of plastic deformation. The general expression is thus

$$f(\boldsymbol{\sigma}) = k \tag{1}$$

where $\boldsymbol{\sigma}$ designates the stress tensor (treated hereafter as a nine-dimensional vector) and k is a characteristic property of the material which may change as the material hardens due to the plastic deformation process.

The expression of the yield criterion can be used to calculate distances between stress points: it is actually a way of defining the *size* of the stress tensor [11,12]. This is really the idea that originated the development of the theory presented here. Let us consider the physical meaning of the two most widely used yield criteria, namely Tresca and Von Mises, as follows. If σ_I, σ_{II} and σ_{III} are the principal stresses, then

$$\tau_I = \frac{1}{2}(\sigma_{II} - \sigma_{II}) \qquad \tau_{II} = \frac{1}{2}(\sigma_{III} - \sigma_I) \qquad \tau_{III} = \frac{1}{2}(\sigma_I - \sigma_{II}) \tag{2}$$

are the principal shear stresses. According to Tresca's rule, plastic strain takes place when the absolute value of either τ_I, τ_{II} or τ_{III} rises to a certain value. Furthermore, it can be shown that the expression of von Mises criterion is equivalent to stating that plastic strain begins when $\tau_I^2 + \tau_{II}^2 + \tau_{III}^2$ rises to another characteristic value. Now, recalling the concept of *norm* on a vector space(see [13], page 4), both criteria can be understood as establishing that plastic flow occurs when the norm of the shear stress vector reaches a certain characteristic value. In the first case the magnitude is measured according to the *maximum norm* $\|\bullet\|_\infty$, whereas in the second the more familiar *Euclidean norm* $\|\bullet\|_2$ is used. This introduces the idea of norm, or more generally, of *distance* in stress space into the theory.

2.2. Flow rule

The flow rule gives the direction of the plastic strain increment. The most widely used theory for this purpose is the associated normality rule, which establishes that the plastic strain increment should be directed along the normal to the yield or loading surface:

$$\mathrm{d}\boldsymbol{\varepsilon}^p = \frac{1}{h}\boldsymbol{n}(\mathrm{d}\boldsymbol{\sigma}\cdot\boldsymbol{n}) \tag{3}$$

where $\mathrm{d}\boldsymbol{\varepsilon}^p$ is the plastic strain increment, $\mathrm{d}\boldsymbol{\sigma}$ the stress increment, $\boldsymbol{n}$ the unit vector normal to the yield surface and h is the so-called *plastic modulus,* an obvious generalization of the notion of plastic modulus in the uniaxial stress-strain curve [9].

2.3. Hardening condition

This condition sets the way the loading surface evolves as plastic strain increases. If the material hardens identically in all directions, then it is said to undergo *isotropic hardening*. In such a case, the variable k in Eq. (1) will be a function of a certain measure of the acumulated plastic strain, such as the plastic work:

$$f(\boldsymbol{\sigma}) = \varphi(W_P) \tag{4}$$

$$W_P = \int_l \boldsymbol{\sigma}\cdot\mathrm{d}\boldsymbol{\varepsilon}^p \tag{5}$$

On the other hand, if a directional effect such as the Bauschinger effect exists, then the material hardens in the direction of the strain and softens in the opposite direction; this behaviour is more accurately modelled by using the so-called *kinematic hardening*, which involves a shift in the loading surface along a certain direction. Mathematically, this is represented by

$$f(\boldsymbol{\sigma}-\boldsymbol{\alpha}) = k \tag{6}$$

where $\boldsymbol{\alpha}$, is the the centre of the loading surface, often called the *backstress*. If the loading surface simultaneously moves and expands in stress space, then a more comprehensive scheme, which is a combination of the previous two, is obtained:

$$f(\boldsymbol{\sigma}-\boldsymbol{\alpha}) = \varphi(W^p) \tag{7}$$

More complicated situations, with rotations or even distortions of the yield surface, have been used at times, but normally the hardening rule describes just the variation of $\boldsymbol{\alpha}$, since in the majority of applications even the isotropic hardening is disregarded.

In order to describe the complex behaviour displayed by materials, it is customary in cyclic plasticity theories, to use not just one, but sometimes two (the yield surface proper and a bounding surface) or even a whole family of yield surfaces that move about in stress space. In these cases, the hardening rule must determine the evolution of all the surfaces. Thus, Mróz's rule for his multiple surface model proposes that the direction translation of a surface is

determined by the point on the next surface having the same exterior normal [9]. In this model, each surface has an associated value of the plastic modulus and the magnitude of the translation of the surfaces is obtained from the *consistency condition*, according to which during plastic loading the stress point must always remain on the current loading surface. Two-surface theories use the same type of hardening rules as the multiple surface model, but the variation of the plastic modulus is prescribed analytically as a function of the relative position between the yield and the bounding surface.

A different approach is followed in the hardening theory of Armstrong and Frederick [10]: a non-linear evolution for the translation of the yield surface is obtained through the solution of a differential equation which relates the actual value of translation in a given load step to the increment of plastic strain and to the current position of the surface. In this theory the consistency condition is used to calculate the value of the plastic modulus.

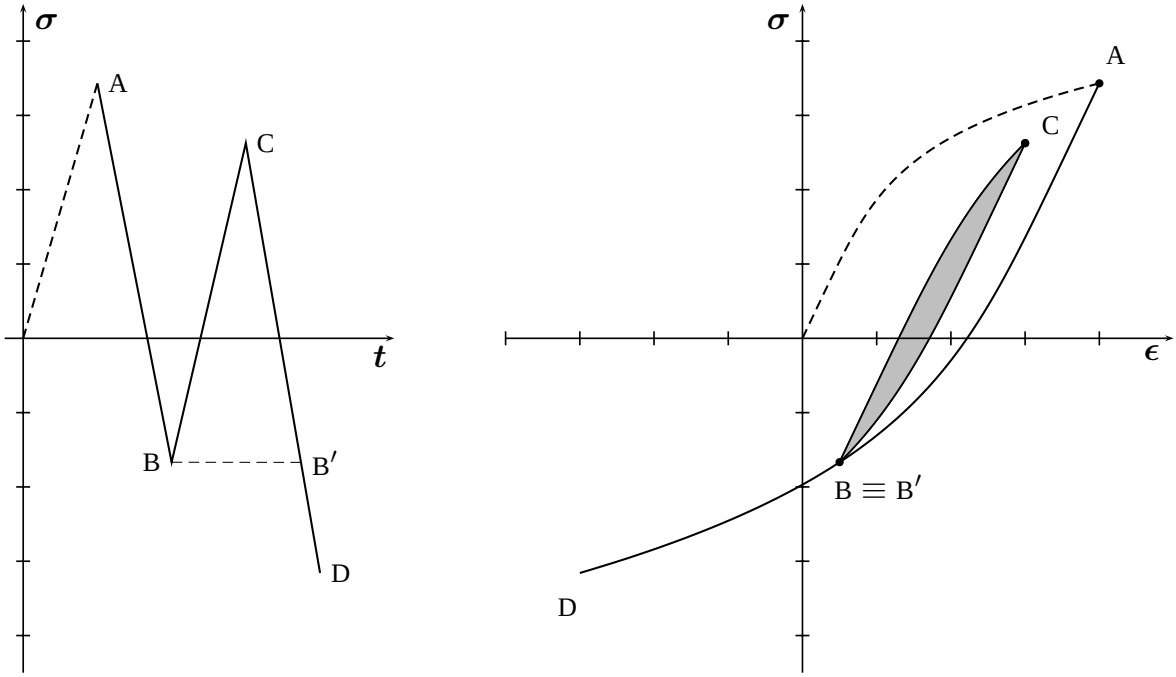

Figure1: Memory effect

2.3 Memory effect

One of the key elements in determining the stress-strain behaviour at the notch root for variable amplitude loading in the Local Strain method is the correct application of the memory effect. This is illustrated in Fig.1, as one moves from point A to D. After reaching point B, the stress is increased to C, following the hysteresis loop. When the load is decreased from C, after reaching point B, the material continues to D along the descending part of the hysteresis loop starting at A, proceeding just as if the small loop B-C-B had never occurred.

This special behaviour of the material "remembering" its deformation path is called *memory effect* [4, 5].

3. THE PROPOSED THEORY

The general concept is that the plastic straining undergone by the material in going from a stress state to another (in "moving between two stress points") depends on the distance between these two stress points. This distance, however, is not to be calculated using the Euclidean norm: the stress space is considered to be a nine dimensional Riemannian vector space.

3.1. Yield criterion: definition of a metric. The fundamental tensor.

If the distance ds between the neighbouring points with coordinates σ^i and $\sigma^i + \mathrm{d}\sigma^i$ is given by the quadratic differential form

$$ds^2 = g_{ij}\, \mathrm{d}\sigma^i \mathrm{d}\sigma^j \tag{8}$$

the space is said to be a Riemannian space (see [14]). The g_{ij}'s are the components of a second order symmetric tensor called the *fundamental tensor* of the space. The quadratic form $g_{ij}\, \mathrm{d}\sigma^i \mathrm{d}\sigma^j$ is called the *metric*. The *magnitude* Q of the vector $\boldsymbol{\sigma}$ with components σ^i is defined by

$$Q^2 = |\sigma|^2 = g_{ij}\, \sigma^i \sigma^j \tag{9}$$

Yielding is simply assumed to occur when the magnitude of the stress vector reaches a given threshold. It is thus expressed

$$Q = |\sigma| = \sqrt{g_{ij}\, \sigma^i \sigma^j} = k \tag{10}$$

The metric of the stress space is thus embedded in the yield criterion.

The structure of the metric tensor turns out to be very simple. One important feature is that the hydrostatic direction must represent a null displacement, i.e., the distance between any two stress points separated only by a hydrostatic stress must be zero. This reflects the fact that hydrostatic stresses do not contribute to yielding. This also ensures that plastic strains do not change volume. By way of example, the metric tensor g_{ij} for a material satisfying the von Mises criterion is given below.

$$g_{ij} = \begin{vmatrix} 1/3 & -1/6 & -1/6 & 0 & 0 & 0 & 0 & 0 & 0 \\ -1/6 & 1/3 & -1/6 & 0 & 0 & 0 & 0 & 0 & 0 \\ -1/6 & -1/6 & 1/3 & 0 & 0 & 0 & 0 & 0 & 0 \\ 0 & 0 & 0 & 1/2 & 0 & 0 & 0 & 0 & 0 \\ 0 & 0 & 0 & 0 & 1/2 & 0 & 0 & 0 & 0 \\ 0 & 0 & 0 & 0 & 0 & 1/2 & 0 & 0 & 0 \\ 0 & 0 & 0 & 0 & 0 & 0 & 1/2 & 0 & 0 \\ 0 & 0 & 0 & 0 & 0 & 0 & 0 & 1/2 & 0 \\ 0 & 0 & 0 & 0 & 0 & 0 & 0 & 0 & 1/2 \end{vmatrix} \tag{11}$$

It must be realized that the matrix g_{ij} is a singular one. The following ordering has been chosen to identify the usual components of the stress tensor and the indices in the nine-dimensional vector space above: $1-\sigma_{11}$, $2-\sigma_{22}$, $3-\sigma_{33}$, $4-\sigma_{12}$, $5-\sigma_{21}$, $6-\sigma_{13}$, $7-\sigma_{31}$, $6-\sigma_{23}$, $9-\sigma_{32}$

3.2. Hardening condition and flow rule

The central hypothesis of the model is that the plastic deformation undergone in moving from a point in the stress space to a different one depends only on the distance between the two as measured with the metric introduced above.

The reference point for the virgin material on application of the first load is the origin of the stress space. In this case, the distance from the origin is the magnitude of the stress vector itself. A hypersphere centred at the origin is the locus of all the points located at the same distance from the origin. It is assumed that the material would have reached the same state of hardening in any of those points. Consider a stress increment $\mathrm{d}\boldsymbol{\sigma}$ from a point in the above-mentioned hypersphere and pointing in the outward direction. This is a loading process. Unloading processes, involving load reversals, are considered later on. Only the component of $\mathrm{d}\boldsymbol{\sigma}$ in the direction $\boldsymbol{n}$ normal to the sphere will increase the distance to the origin. Accordingly, the plastic strain caused by $\mathrm{d}\boldsymbol{\sigma}$ will develop in that normal direction. Its modulus will be given by the increment of a certain *hardening function* $\lambda(\bullet)$, a scalar function whose argument is the separation between the stress points. As long as a loading process progresses, the distance is measured between the current stress point and the point where that loading excursion started, and this distance is the argument of the hardening function. When unloading occurs, an essential difference arises as discussed below. Since $Q = |\sigma|$ designates the distance to the origin during the first loading process, the reasoning above establishes the flow rule by means of the following equations

$$\left|\mathrm{d}\boldsymbol{\varepsilon}^{p}\right| = \mathrm{d}\lambda = \frac{\mathrm{d}\lambda}{\mathrm{d}Q}\mathrm{d}Q = \Phi(Q)\mathrm{d}Q \tag{12}$$

and

$$\mathrm{d}\boldsymbol{\varepsilon}^p = \Phi(Q)\mathrm{d}Q\,\boldsymbol{n} \tag{13}$$

where $\Phi(Q)$, the derivative of the hardening function, will be called hereafter the *hardening modulus*. Further details of the above rules can be obtained in [15]. The hardening function can be very easily derived from conventional tests. For example, the analytical procedure for establishing the hardening function for a Ramberg-Osgood material is similar to that described in [11].

The unit normal vector $\boldsymbol{n}$ is obviously calculated through the gradient of Q:

$$\boldsymbol{n} = \frac{\nabla Q}{|\nabla Q|} \tag{14}$$

The gradient of Q is a (nine-dimensional) vector whose components are the partial derivatives of Q with respect to the σ^i components. It is said to be a *covariant* vector (see [14], page 6). We need not be concerned here with the precise mathematical meaning of this term. It is just mentioned because it is customary to write the components of such vectors with the labels as a subscript, rather than as a superscript, as has been done with the σ^i themselves. It can be shown that $|\nabla Q| = 1$ (see [12]). Therefore,

$$\boldsymbol{n} = \nabla Q \tag{15}$$

and

$$n_i = \frac{g_{ij}\sigma^j}{Q} \tag{16}$$

Note the application of the summation convention in the numerator. This is an example of the process known as *lowering the superscript* [14, page 20]. The increment of Q is then given as

$$\mathrm{d}Q = \nabla Q \cdot \mathrm{d}\boldsymbol{\sigma} = \boldsymbol{n} \cdot \mathrm{d}\boldsymbol{\sigma} \tag{17}$$

Consequently, the flow rule can also be expressed in a more direct way as a function of the stress increment $\mathrm{d}\boldsymbol{\sigma}$:

$$d\boldsymbol{\varepsilon}^p = \Phi(Q)(\mathrm{d}\boldsymbol{\sigma} \cdot \boldsymbol{n})\boldsymbol{n} = \Phi(Q)(\boldsymbol{n} \otimes \boldsymbol{n})\mathrm{d}\boldsymbol{\sigma} \tag{18}$$

where the property that defines the tensor product ($\otimes$) of two vectors has been used[†].

[†] The tensor product $\boldsymbol{a} \otimes \boldsymbol{b}$ of two vectors $\boldsymbol{a}$ and $\boldsymbol{b}$ is the *linear application* that assigns to each vector $\boldsymbol{v}$ the vector $(\boldsymbol{b} \cdot \boldsymbol{v})\boldsymbol{a}$ (see [16], page 4):

$$(\boldsymbol{a} \otimes \boldsymbol{b})v = (\boldsymbol{b} \cdot \boldsymbol{v})\boldsymbol{a}$$

Its components are given as $(\boldsymbol{a} \otimes \boldsymbol{b})_{ij} = a_i b_j$

One can now relate the increment of total strain to the increment of stress by simply adding the elastic strain, which is introduced by means of the Hook tensor H . The expression is

$$\mathrm{d}\boldsymbol{\varepsilon} = (H + \Phi(Q)(\boldsymbol{n} \otimes \boldsymbol{n}))\mathrm{d}\boldsymbol{\sigma} \tag{19}$$

This important equation represents the instantaneous linear relationships between the stress and strain increments which are needed in numerical calculations. It can be shown that they are equivalent to the well-known Prandtl-Reuss equations of plastic flow if the von Mises metric is used.

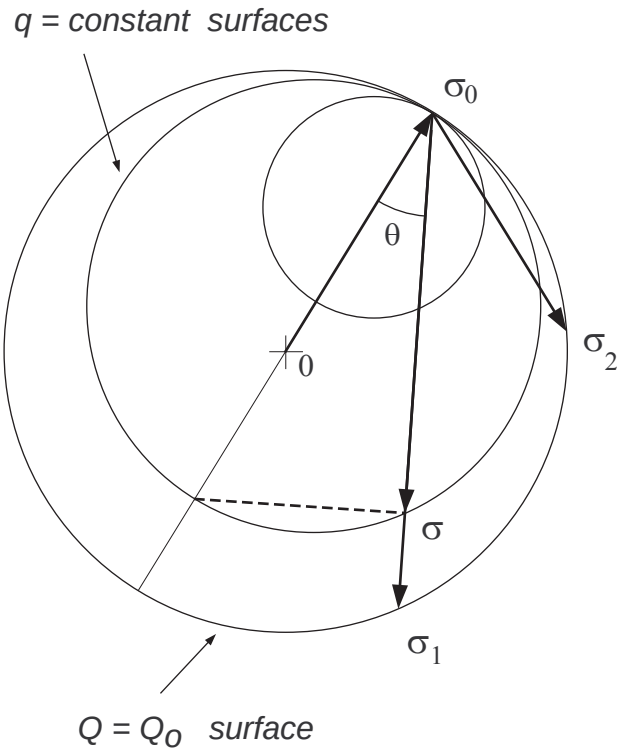

Figure 2: Measuring distances after unloading

Let us now analyse what happens after unloading is detected. Unloading would occur in a certain load step if $\mathrm{d}Q \le 0$, i.e., if Q were to decrease in that load step. That would signal the starting of a new load excursion along a new hysteresis loop, using the Local Strain terminology, so to speak. Imagine that the material has been loaded as far as point $\boldsymbol{\sigma}_0$ at a distance Q_0 from the origin. Based on the previous reasoning, the same degree of hardening would correspond to every point on the surface $Q = Q_0$ (see Fig. 2). Let us compare the unloading from $\boldsymbol{\sigma}_0$ to points such as $\boldsymbol{\sigma}_1$ and $\boldsymbol{\sigma}_2$ on the same surface. On moving from $\boldsymbol{\sigma}_0$ towards $\boldsymbol{\sigma}_1$ or $\boldsymbol{\sigma}_2$ the value of Q measured relative to the origin will initially decrease and, hence, unloading will be detected. As movement proceeds, in both cases Q will decrease and then increase to its original level. The way in which Q evolves will be very different in the two cases, yet the final state of hardening should be the same, since the original surface is

reached again. Once more, measuring distances between $\boldsymbol{\sigma}_1$ and $\boldsymbol{\sigma}_0$ and between $\boldsymbol{\sigma}_2$ and $\boldsymbol{\sigma}_0$ render different values, and yet the degree of hardening is the same. Since our basic assumption is that hardening depends on distance between stress points, we come to the conclusion that, on load reversals, distances must be calculated differently: all paths such as those in Fig. 2, beginning and ending in the same sphere (and through its interior), must have the same *length* from the point of view of hardening and this *length* must be the argument of the hardening function under unloading conditions. We, thus, speak of a generalized distance or separation on unloading and equate it to the diameter of the hypersphere that contains the end points.

Based on this definition, the generalized distance q between two points $\boldsymbol{\sigma}$ and $\boldsymbol{\sigma}_0$ would simply be given as

$$q = \frac{|\boldsymbol{\sigma} - \boldsymbol{\sigma}_0|}{\cos\theta} \tag{20}$$

where θ is the angle between the upward and downward trajectories depicted in Fig. 2. The term $\cos\theta$ is calculated with usual formula through the scalar product of $\boldsymbol{\sigma} - \boldsymbol{\sigma}_0$ and $-\boldsymbol{\sigma}_0$,

$$\cos\theta = \frac{(-\boldsymbol{\sigma}_0)\cdot(\boldsymbol{\sigma} - \boldsymbol{\sigma}_0)}{|\boldsymbol{\sigma}_0||\boldsymbol{\sigma} - \boldsymbol{\sigma}_0|} \tag{21}$$

Note carefully that the scalar product must be calculated by means of the fundamental tensor (see [16], page 20-21),

$$-\boldsymbol{\sigma}_0 \cdot (\boldsymbol{\sigma} - \boldsymbol{\sigma}_0) = -g_{ij}\sigma_0^i(\sigma^j - \sigma_0^j) \tag{22}$$

In this case, the unloading iso-hardening surfaces will be hyperspheres tangential at $\boldsymbol{\sigma}_0$. It is interesting to compare Fig. 2 with the classic experimental data of Lamba and Sidebottom [1], as well as with the representations of the Mróz multisurface model [9]. Note how in Mróz's model the yield surfaces are tangent at the current stress point, whereas here the surfaces are tangent at the point where the current loading process started.

If loads change direction in succession, then the distance q is obtained by projecting onto the diameter of the hardening surface which contains the last two points of load reversal (see Fig. 3). In this case one has

$$\cos\theta = \frac{(\boldsymbol{\sigma}_{ca} - \boldsymbol{\sigma}_i)\cdot(\boldsymbol{\sigma} - \boldsymbol{\sigma}_i)}{|\boldsymbol{\sigma}_{ca} - \boldsymbol{\sigma}_i||\boldsymbol{\sigma} - \boldsymbol{\sigma}_i|} \tag{23}$$

where $\boldsymbol{\sigma}_{ca}$ is the centre of the above-mentioned loading surface and $\boldsymbol{\sigma}_i$ the starting point for the segment.

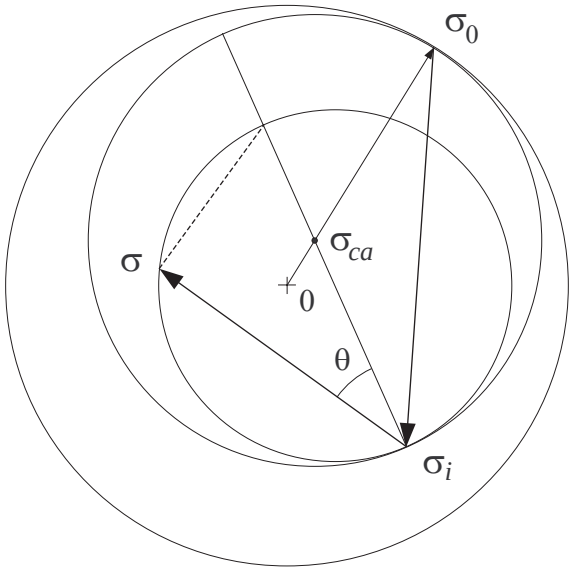

Figure 3: Successive change of loading direction

Under these conditions, the flow rule is defined by an expression similar to that used for the first loading case,

$$\mathrm{d}\boldsymbol{\varepsilon}^p = \phi(q)\mathrm{d}q\,\boldsymbol{n} \tag{24}$$

The hardening modulus function $\phi(q)$ is calculated from a cyclic test, but this time from the hysteresis loops rather than from the cyclic curve. With materials of the Masing type, the hysteresis loop is determined simply by scaling the cyclic behaviour curve by a factor of 2, so the relationship between $\Phi(q)$ and $\phi(q)$ is very simple: $\phi(q)=\Phi(Q=q/2)$. The vector $\boldsymbol{n}$ in the equation above is now given by the gradient of q. The magnitude of the gradient of q can be shown to be $1/\cos^2\theta$, so the expression of the flow rule reduces to

$$d\boldsymbol{\varepsilon}^p = \phi(Q)\frac{1}{\cos^2\theta}(\boldsymbol{n}\otimes\boldsymbol{n})\,\mathrm{d}\boldsymbol{\sigma} \tag{25}$$

and vector $\boldsymbol{n}$ has the form

$$\boldsymbol{n} = \frac{2}{q}(\boldsymbol{\sigma}-\boldsymbol{\sigma}_i) - \frac{2}{q_{i-1}}(\boldsymbol{\sigma}_{ca}-\boldsymbol{\sigma}_i) \tag{26}$$

where q_{i-1} is the diameter of the loading surface where $\boldsymbol{\sigma}_i$ lies.

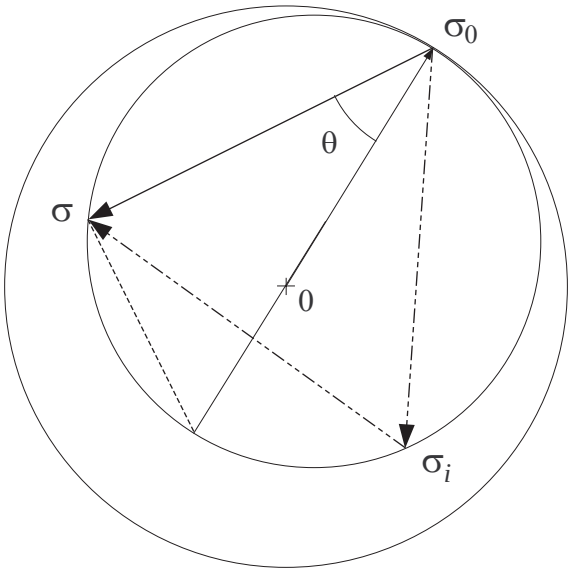

Figure 4: Memory effect (multiaxial case)

3.3. Multiaxial memory rule

The memory effect appears in very simple terms in the present framework. Consider a loading process involving several reversals such as that of Fig. 3. Imagine that $\boldsymbol{\sigma}$ keeps moving away from $\boldsymbol{\sigma}_i$: a point would be reached where q would equal the diameter of the surface where the starting point for that particular loading segment is inscribed (see Fig. 4). At that point, it is assumed that a cycle is closed and from then on the material behaves as though such a cycle had never occurred. Thus, if the distance q was until then being measured relative to $\boldsymbol{\sigma}_i$ and projecting onto the diameter joining $\boldsymbol{\sigma}_i$ and $\boldsymbol{\sigma}_{ca}$, beyond that point it is again measured with respect to $\boldsymbol{\sigma}_0$, and by projecting onto the diameter through the origin and $\boldsymbol{\sigma}_0$. Should the phenomenon take place in deeper nested surfaces, the effect would be similar. Note that, at the time a given cycle closes, the expanding surface and the reference one coincide, so they share the same normal at $\boldsymbol{\sigma}$ and continuity in the plastic strain is guaranteed.

3. APPLICATION TO EXPERIMENTAL RESULTS

This section discusses the application of the proposed model to experimental results reported by Lamba and Sidebottom [1] on a tubular specimen of oxygen-free high-conductivity (OFHC) copper subjected to combined tension and torsion. The specimen was subjected to torsional cycling and then to 90 deg out-of-phase cycling until it fully stabilized. A comparison made between axial, torsional and out-of-phase cycling for this material showed that the cyclic hardening produced by out-of-phase cycling was appreciably greater. Therefore, in the calculations reported here, the out-of-phase hardening has been taken into

account by the simplest procedure of obtaining the hardening modulus function from the effective stress versus effective strain curve derived in 90 deg out-of-phase experiments. This is the procedure followed by McDowell et al. [17] on their analysis of the same experimental data. In fact, the stable effective cyclic stress-strain curve used here, and shown in Fig 5, is the one presented by McDowell (see his figure 5b), which has been approximated as piecewise linear by means of 7 segments.

In the specimen under study here, when the stress response stabilized, the strain levels were continuously decreased in the same out-of-phase manner until all the stresses and strains were reduced to zero. Following this, the non-proportional strain path in Fig. 6 was imposed. According to the authors, this strain path was chosen because it includes a wide range of angles between different paths segments and because the path had equal positive and negative peaks.

The end points of the path segments were numbered from 0 to 8 and the path was traversed in a numerically increasing sequence (Fig. 6). The stress and strain response of the material to the nonproportional path appears in Fig. 7 and can be seen to be quite complex.

The stresses and strains at each end of the loading cycle are shown in Table 1, along with the values predicted by the theory presented here. This table is adapted from that presented by McDowell. For the sake of comparison, predictions effected by Lamba and Sidebottom and by McDowell are also included in the table. Lamba and Sidebottom's model used two Tresca surfaces and the Mróz infinitesimal kinematic hardening rule. The nonlinear strain hardening behaviour assumption was that the stress-plastic strain slope was an exponential function of the distance between the stress point and the point on the limit surface having the same exterior normal, and the stress-strain slope was taken to be zero on the limit surface. McDowell's model used up to 13 Tresca surfaces with effective strain increments ranging from 0.01 to 0.45 percent and the Garud finite increment hardening rule. Note that the present model predicts the biaxial response as accurately as the others. The average error in predicted axial and shear stresses at the designated points 0-8 of the loading cycle is around 15% for the three studies.

It is thus justified to use words similar to those of Lamba and Sidebottom and to say that *when the experimental results and the present formulation's prediction are compared, the striking similarity is unmistakable. All path segments are faithfully predicted and the quantitative agreement is reasonably good.* This seems to be a fair performance for a model that only requires to solve in each load step a *linear* relationship between the stress and strain increments and to check for the closure of "hysteresis loops" for application of the memory rule in much the same way as has become customary in the Local Strain Approach.

Acknowledgements

The author gratefully acknowledge the financial support for this investigation provided by the Spanish DGICYT through project DPI2005-04077.

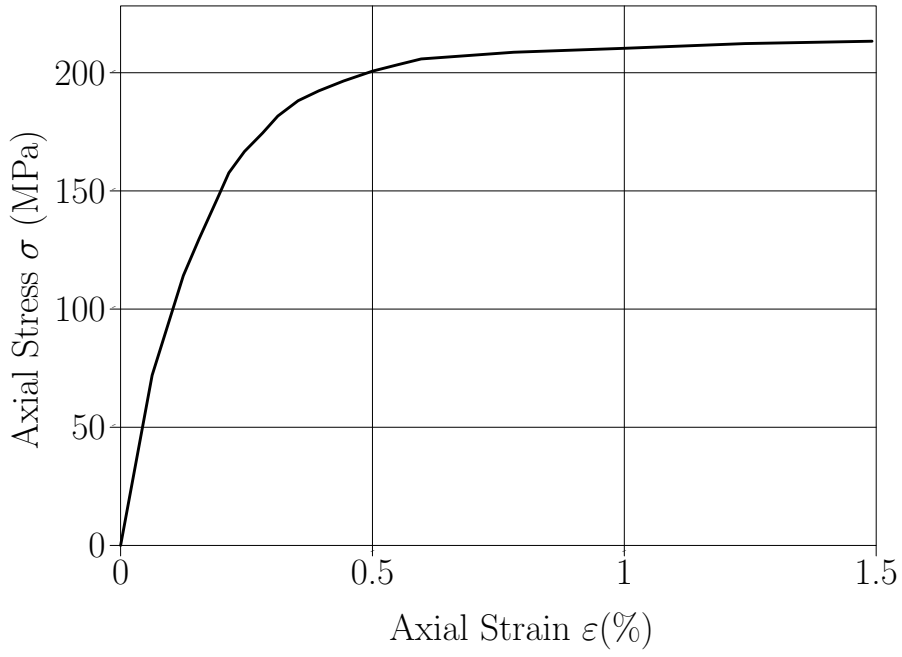

Figure 5: Stress-strain curve used to obtain the hardening modulus function

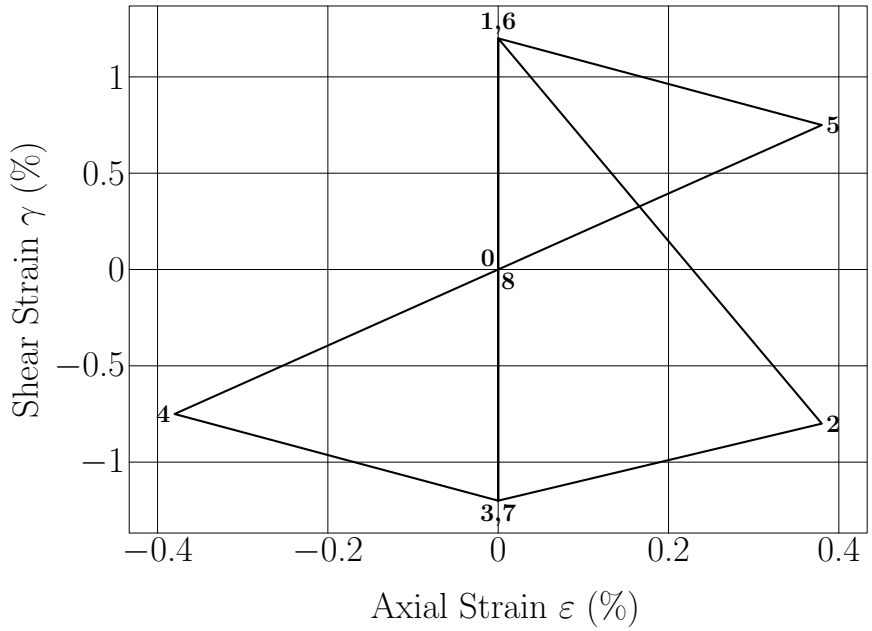

Figure 6: Imposed strain history

Table 1: Comparison of experimental and predicted values

	Strain Path		Mc Dowell Study[17]				Lamba Study[1]				This Study				Experiment	
Point	∈ (%)	γ (%)	σ (MPa)	Error (%)	τ (MPa)	Error (%)	σ (MPa)	Error (%)	τ (MPa)	Error (%)	σ (MPa)	Error (%)	τ (MPa)	Error (%)	σ (MPa)	τ (MPa)
0	0	0	0	--	0	--	0	--	0	--	0	--	0	--	0	0
1	0	1.2	0	--	99	3.03	0	--	95	6.86	0	--	119.25	-16.91	0	102
2	0.38	-0.8	65	19.75	-95	-4.21	66	22.73	-93	-2.20	65.1	19.63	-112	-23.08	81	-91
3	0	-1.2	-163	-28.35	-58	46.55	-160	-20.63	-65	23.53	-163.4	-28.66	-75.8	10.82	-127	-85
4	-0.38	-0.75	-172	8.02	51	-7.84	-193	-3.11	39	17.02	-185.7	0.70	60.1	-27.87	-187	47
5	0.38	0.75	143	-30.00	70	18.57	145	-24.14	73	12.05	143.2	-30.18	95.4	-14.94	110	83
6	0	1.2	-157	-2.61	60	30.00	-128	19.53	74	5.13	-156.4	-2.22	91.3	-17.05	-153	78
7	0	-1.2	0	--	-100	3.00	0	--	-93	9.71	-11.7	--	-113.6	-10.29	0	-103
8	0	0	0	--	99	-4.04	0	--	88	7.37	-10.23	--	102.82	-8.23	0	95

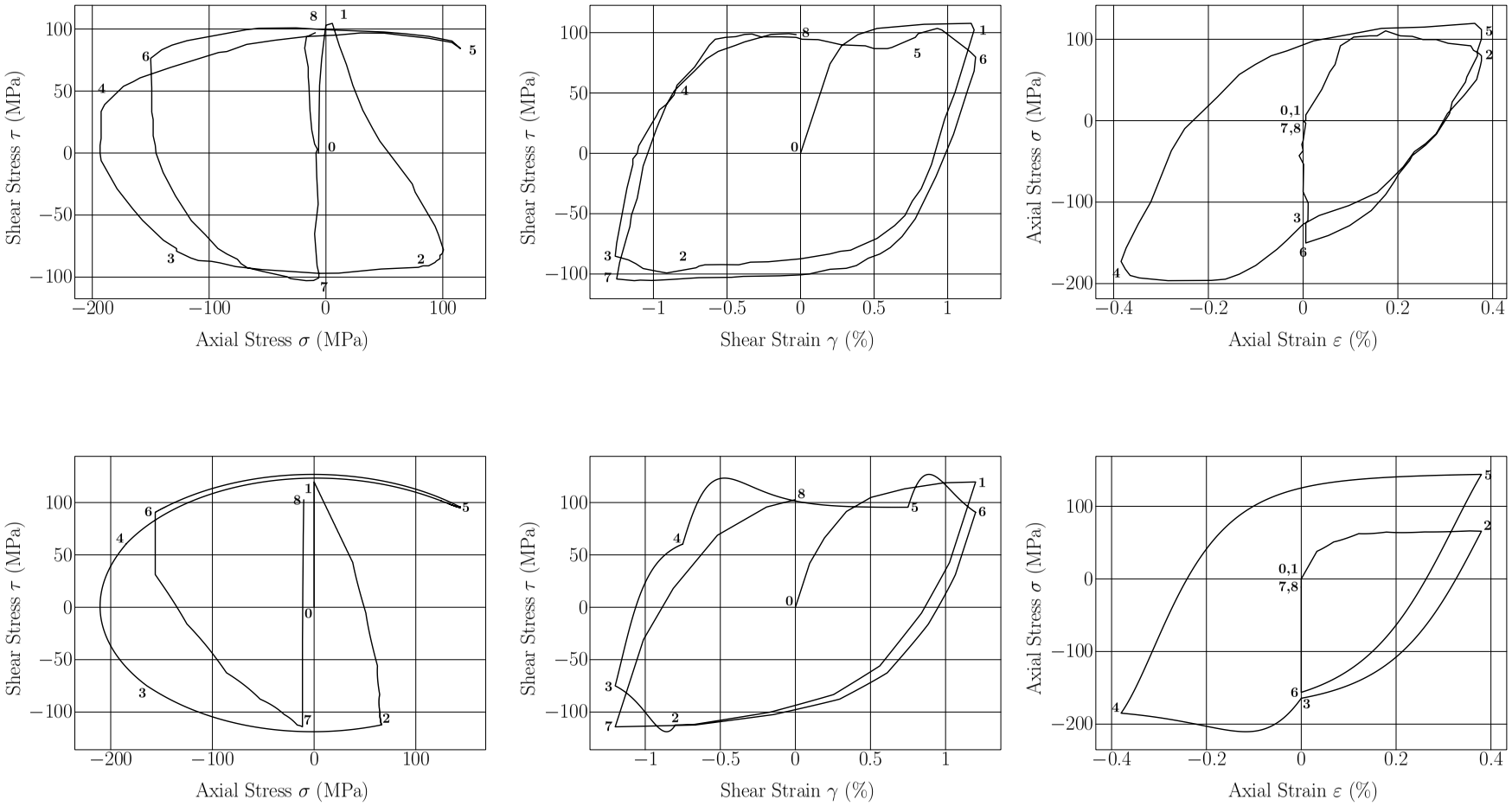

Figure 7: Comparison of experimental (upper row) and predicted (lower row) results

References

[1] Lamba, H. S., Sidebottom, O. M. (1978) Cyclic Plasticity for Non-proportional Paths: Parts 1and 2, ASME Journal Of Engineering Materials and Technology, **100**, 96-103 and 104-111.

[2] MSC.Fatigue, MSC Software Corporation.

[3] FE-Fatigue, nCode International.

[4] Dowling, N.E. (1993) Mechanical Behaviour of Materials. Engineering Methods for Deformation, Fracture and Fatigue. Prentice Hall, Inc.

[5] Bannantine, J. A., Comer, J.J., Handrock, J.L. (1990) Fundamentals of Metal Fatigue Analysis, Prentice Hall, Inc.

[6] Hoffman, M., Seeger, T. A (1985) A Generalized Method for Estimating Multiaxial Elastic-Plastic Notch Stresses and Strains, Part 1: Theory", ASME Journal Of Engineering Materials and Technology, **107**, 250-254.

[7] Glinka, G., Buczyński, A. Ruggeri, A. (2000) Elastic-plastic Stress-Strain Analysis of Notches under Non-Proportional Loadings Paths, Archives of Mechanics, **52**, 4-5, 589-607.

[8] Socie, D. F., Marquis, G. B. (2000) Multiaxial Fatigue, Society of Automotive Engineers, Inc.

[9] Mróz, Z. (1967) On the Description of Anisotropic Workhardening, Journal of the Mechanics and Physics of Solids, **15**, 163-175.

[10] Armstrong, P. J., Frederick, C. O. (1966) A Mathematical Representation of the Mualtiaxial Bauschinger Effect, C.E.G.B. RD/B/N 731, 1966.

[11] Navarro, A., Brown, M.W., Miller, K.J. (1993) A Multiaxial Stress-Strain Analysis for Proportional Cyclic Loading, Journal of Strain Analysis for Engineering Design, **28**, 2, 125-133.

[12] Navarro, A., Brown, M.W. (1997) A Constitutive Model for Elasto-Plastic Deformation under Multiaxial Straining, Fatigue and Fracture of Engineering Materials and Structures, **20**, 5,747-758.

[13] Isaacson, E. Keller, H.B. (1994) Analysis of Numerical Methods, Dover Publications, Inc.

[14] Spain, B. (2003) Tensor Calculus. A Concise Course. Dover Publications, Inc.

[15] Navarro, A., Giráldez, J. M., Vallellano, C. (2005) A Constitutive Model for Elastoplastic Deformation Ander Variable Amplitude Multiaxial Cyclic Loading, Accepted for publication in the Internacional Journal of Fatigue.

[16] Gurtin, M.E. (1981) An Introduction to Continuum Mechanics, Academic Press, Inc.

[17] McDowell, D.L., Socie, D.F. and Lamba, H.S. (1982) Multiaxial Nonproportional Cyclic Deformation, *Low Cycle Deformation and Life Prediction, ASTM STP 770,* C. Amzallag, B.N. Leis and P. Rabbe, Eds., American Society for Testing and Materials, pp. 500-518.